Review

Coarse-Grained Protein Dynamics Studies Using Elastic Network Models

Yuichi Togashi [1,2,3,]* and **Holger Flechsig** [4]

1   Research Center for the Mathematics on Chromatin Live Dynamics (RcMcD), Department of Mathematical
     and Life Sciences, Graduate School of Science, Hiroshima University, 1-3-1 Kagamiyama,
     Higashi-Hiroshima, Hiroshima 739-8526, Japan
2   RIKEN Center for Biosystems Dynamics Research (BDR), 6-2-3 Furuedai, Suita, Osaka 565-0874, Japan
3   Cybermedia Center, Osaka University, 5-1 Mihogaoka, Ibaraki, Osaka 567-0047, Japan
4   Nano Life Science Institute (WPI-NanoLSI), Kanazawa University, Kakuma-machi, Kanazawa,
     Ishikawa 920-1192, Japan; flechsig@staff.kanazawa-u.ac.jp
*   Correspondence: togashi@hiroshima-u.ac.jp; Tel.: +81-82-424-7373

check for
updates

Abstract: Elastic networks have been used as simple models of proteins to study their slow structural dynamics. They consist of point-like particles connected by linear Hookean springs and hence are convenient for linear normal mode analysis around a given reference structure. Furthermore, dynamic simulations using these models can provide new insights. As the computational cost associated with these models is considerably lower compared to that of all-atom models, they are also convenient for comparative studies between multiple protein structures. In this review, we introduce examples of coarse-grained molecular dynamics studies using elastic network models and their derivatives, focusing on the nonlinear phenomena, and discuss their applicability to large-scale macromolecular assemblies.

1. Introduction

Cells are made up of soft materials, and proteins are one of the major components of cells. Besides unfolded and intrinsically disordered proteins, many folded proteins show large-amplitude motions (transitions) between ensembles of conformations. Such conformational motions are often related to their functional cycles such as reactions in enzymes or the translocation of ions in transporters. Hence, to fully understand the mechanism of action of proteins, it is important not only to elucidate their static structures but also to understand their dynamic and mechanical aspects.

A large number of experimental studies have focused on the elucidation of the dynamic and mechanical aspects of various proteins. Nuclear magnetic resonance (NMR) can provide valuable information about protein structures in solution, including their fluctuations. Owing to the recent developments in cryo-electron microscopy (cryo-EM) techniques, realistic structures in solution can now be observed at a high resolution. Atomic force microscopy (AFM) can even visualize the motion of each protein in physiological conditions as a molecular movie [1,2]. It is, however, difficult to pursue both live motion at a high temporal resolution (using a high enough frame rate) and high spatial resolution in a single experiment. This emphasizes the important role of numerical simulations, to integrate and interpret experimental results.

Molecular dynamics (MD) has been used to investigate the motion and mechanical properties of proteins for over 40 years [3]. The accessible time-scale of an all-atom MD for a small protein has been

extended from picoseconds to milliseconds [4]. Even complex cytoplasmic environments [5] or whole virus capsids [6] have been modeled and simulated. However, operation cycles of protein machines are slow, typically taking milliseconds to seconds. Even using state-of-the-art supercomputers, all-atom MD simulations beyond the timespan of seconds are currently not realistic. Moreover, due to thermal and hydrodynamic fluctuations at the nano-scale, the operation of proteins is non-deterministic, demanding statistical analyses over a number of functional cycles and simulation trials.

Hence, we still need to reduce the computational cost of molecular dynamics simulations, by coarse-graining and simplification of the model. There is already a huge variety of coarse-grained models for structural dynamics of proteins, at the sub-residue level (e.g., MARTINI [7]), residue level (e.g., many Gō-like models [8–10], AICG and variants [11,12]), even coarser or multiscale [13]. Force fields are simplified in different ways in each of these models.

One of the simplest among them is the elastic network model (ENM), in which all the interactions are simplified as springs obeying Hooke's law. As the interaction potential (force field) depends on a reference structure, ENMs could be seen as a variant of Gō-like models. Despite the radical simplification, ENMs could provide insights into slow conformational motions and relate them to the function of proteins. It is possible to reproduce conformational changes over entire operation cycles. Because of their low computational costs, ENMs are also convenient for comparative studies of many different protein structures. In this review, we briefly explain ENMs and their features, and introduce examples of MD studies using ENMs contributed by us and other groups. We also discuss the improvements in modeling, and further applications beyond single proteins.

2. Background

2.1. Elastic Network Models

ENMs consist of point-like particles and linear (Hookean) springs connecting the particles. When adopted as a model of a protein, the particles are placed according to a given reference structure of the protein, and then the pattern of connections (springs) is determined by a certain rule. In the simplest form, the network is constructed as follows. To determine the connectivity, the distance between each pair of particles in the reference structure is calculated, and if that value is less than a certain cutoff distance, the pair is connected by a spring; all the springs have the same stiffness constant. The equilibrium length of each spring is set equal to the corresponding distance between the particles in the reference structure so that the reference structure always corresponds to the minimum energy (most stable) state.

The original ENM for proteins by Tirion [14] was an atomic model where each atom is represented by a particle (see also [15]). Coarse-grained ENMs, in which each amino-acid residue is represented by a particle, were then suggested and broadly used [16,17]. To construct a coarse-grained ENM, we usually substitute each α-carbon atom in the reference structure with a particle, and set the cutoff distance $\sim$10 Å [18]. Below, we use the term ENM for coarse-grained ENMs unless specified. For the mathematical representation, see Appendix A.1.

There are two ways in which ENMs are commonly represented and analyzed: Gaussian network models (GNM) and anisotropic network models (ANM).

If we focus only on fluctuations around the reference structure, and assume that the fluctuations are isotropic, the behavior can be described by the intensity of fluctuations of each particle (regardless of the direction in which the particle fluctuates). Then, the conformational space of the model (with N particles) is reduced to be N-dimensional (i.e., the directions are lost and only the magnitudes of their displacement are available). The models in this class are called Gaussian network models (GNM), as the isotropic Gaussian form of fluctuations are assumed. They are used for normal mode analysis (NMA; see Section 2.2) to estimate overall fluctuations at each part of the molecule. In the linear regime, the dynamics can be represented by an $N \times N$ matrix derived from the connectivity and stiffness.

Although the idea of GNM dates back further [19,20], these models were constructed according to an experimentally known structure when applied to proteins.

If we also need the direction in which each particle moves (in 3-dimensional real space), then the conformational space is $3N$-dimensional as the (x,y,z)-displacement of each particle is considered. The direction of the force induced by a spring coincides with the direction of the spring, and the intensity of the force is determined by the change in spring length, which is affected by displacement of the particles connected by the springs. Such models are called anisotropic network models (ANM), and are also analyzed by NMA [21,22].

2.2. Normal Mode Analysis

To investigate fluctuations or structural transitions in ENMs, NMA is often adopted. In NMA, the motion is linearly approximated around the steady state (i.e., the force on each particle is represented by only the first order of displacement; see Equation (A7) in Appendix A.2), and then decomposed into mutually orthogonal normal modes. This decomposition is mathematically executed by solving the eigenvalue problem of the linearization matrix (i.e., Hessian matrix of the elastic potential energy, scaled by mass or mobility); each eigenvalue shows the frequency (in underdamped cases) or decay rate (in the overdamped limit) of the motion toward the direction of the corresponding eigenvector. Particular focus is on those modes with small eigenvalues, as they represent soft and slow (often large amplitude) motion, typically overdamped in solution [23].

NMA is a general method and has been widely used in molecular mechanics studies along with all-atom models [24–28]. There are several advantages of ENMs when used within the framework of NMA. By definition, the reference structure is always (one of) the state(s) of minimum energy, and thus energy minimization before the analysis is not required. When NMA is applied to GNMs, the $N \times N$ connectivity matrix (the Kirchhoff matrix) can be directly used as the linearization matrix.

The dynamics of ANMs in the linear regime is represented by a $3N \times 3N$ matrix. In contrast to GNMs, the linearization matrix includes information not only on the connectivity and stiffness but also on the directions of the springs in the reference structure (see Appendix A.2). The force induced by each spring in the linear regime is only toward the direction of the spring in the reference structure, and the intensity is linear to each of x, y, or z-displacement of the particles connected to the spring. Hence, the linearization matrix can be easily obtained (see Equation (A9)).

Since the 1990s, GNM-NMA has been applied to a variety of protein structures, and has successfully reproduced fluctuations of each residue observed in experiments (e.g., the pattern of B-factors obtained from crystallography). Later, ANM-NMA was introduced, and in addition to reproducing the overall intensity of fluctuations, it has been evidenced that the direction of a single (or a few) slow normal modes agreed well with structural changes between two or more known structures at different states (e.g., ATP-bound and ATP-free states in the functional cycle) in protein machines. Owing to its simplicity and extremely low computational costs, these methods became increasingly popular to identify functional conformational motions in protein machines and motors (e.g., with GNM [29–32] and ANM [30–34]). There are also automated online services [35–38] and databases [39,40] available for ENM-NMA (see also variants using dihedral angles as independent variables [41–44]). For details of the methods and further examples, see reviews e.g., [45–51].

2.3. Nonlinearity of ENMs

Although linear NMA could be successfully applied as discussed above, the dynamics of ENMs is intrinsically nonlinear even though all the springs are linear with respect to their deformations (see Appendix A.1). The nonlinearity arises because the direction of each spring, and consequently the direction of the force induced by the spring, can change through the deformation (see Figure A1 for an illustrative case). Hence, for relatively large deformations, the behavior of ENMs may deviate from the prediction by NMA. The linear response approximation strictly holds only as long as the displacements (changes in the Cartesian coordinates) of network particles from their equilibrium

positions are much smaller than the natural lengths of springs. The fact that ENM-NMA for proteins nonetheless describes very well even large-amplitude conformational transitions (which certainly involve large displacements of groups of particles) is remarkable, and may represent a property which is unique to those proteins operating as machines. Still, the validity regime of ENM-NMA in general has to be questioned.
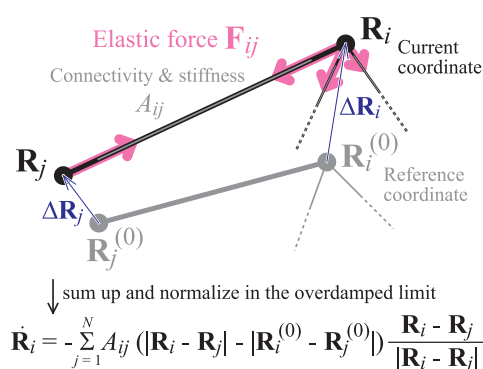
If we consider elastic networks as dynamical systems, their behavior beyond the NMA can be explored. We can perform coarse-grained MD simulations using ENMs, in which each particle is numerically tracked according to Newton's equation of motion. Obviously, the conformational space of the network has $3N$ degrees of freedom (the (x,y,z)-coordinates of each particle). In this approach, the full nonlinear elastic dynamics of the network is considered, and effects of nonlinearity can be discussed.

The nonlinear effect was formerly discussed in the context of transitions between structural states, sometimes involving partial unfolding ("proteinquake") [52]. Attempts were made to connect (interpolate) multiple structures by iteratively applying NMA or introducing a smooth potential surface [53–57]. Also, ENM variants explicitly including nonlinear (higher-order) terms have been developed (e.g., nonlinear network model (NNM) [58]) and used for MD simulations (e.g., [59]).

While the dynamics of compactly folded protein ENMs is intrinsically nonlinear, the question is also to what extent the harmonic restraints between particles in protein ENMs keep their validity. If, e.g., local deformation (strain) of springs is excessive, ENMs are not able to capture possible processes of unfolding. However, if the molecule is sufficiently large, it is possible that its overall deformation is large while local deformation remains very small. In such cases, NMA may break down in the regime where monolithic ENMs (without any interpolation or correction) are still good approximations. Because of the nonlinearity, MD simulations using ENMs may provide additional information beyond the NMA.

2.4. ENM-MD Simulations

To consider the effects of nonlinearity, we performed coarse-grained MD simulations using ENMs and compared the trajectories with the results of ANM-NMA [60,61]. Each particle in the network follows Newton's equation of motion, and the temporal evolution of the network is obtained by numerically integrating the set of coupled equations. When the focus is on slow conformational motion in proteins, inertial effects can be omitted [23], and the equations of motion are considered in the overdamped limit (i.e., the velocity of the particle is proportional to the sum of the forces acting on it; see Figure 1 and Appendix A.1).

$$\dot{\mathbf{R}}_i = -\sum_{j=1}^{N} A_{ij} \left(|\mathbf{R}_i - \mathbf{R}_j| - |\mathbf{R}_i^{(0)} - \mathbf{R}_j^{(0)}| \right) \frac{\mathbf{R}_i - \mathbf{R}_j}{|\mathbf{R}_i - \mathbf{R}_j|}$$

Figure 1. Schematic diagram of the elastic network model (ENM). Each spring (i, j) obeys Hooke's law; i.e., the strength of its elastic force $\mathbf{F}_{ij}$ is proportional to its deformation from the equilibrium length, and the force direction coincides with the spring direction. The resultant force $\mathbf{F}_i$ on particle i is the sum of forces $\mathbf{F}_{ij}$ exerted by all the springs connected to the particle. In dynamic simulations in the overdamped limit (Section 2.4), the velocity $\dot{\mathbf{R}}_i$ of particle i is directly calculated from $\mathbf{F}_i$. Adapted from [62].

Figure 2 shows examples of two different classes of molecular motors: myosin V and kinesin KIF1A [61]. Starting from random deformations, in most cases, the trajectories quickly converge to an energetic valley, and slowly go back along the valley to the reference conformation. If we start from the conformation in another state, we can simulate the transition between the states (e.g., if the ENM is constructed according to the ligand-bound state and the simulation starts from the ligand-free conformation, then the simulation mimics the motion after ligand binding). Also in this case, the trajectories go along a well-defined pathway and are robust against fluctuations. In both cases, the behavior at the final stage agrees with the slowest mode in the NMA.
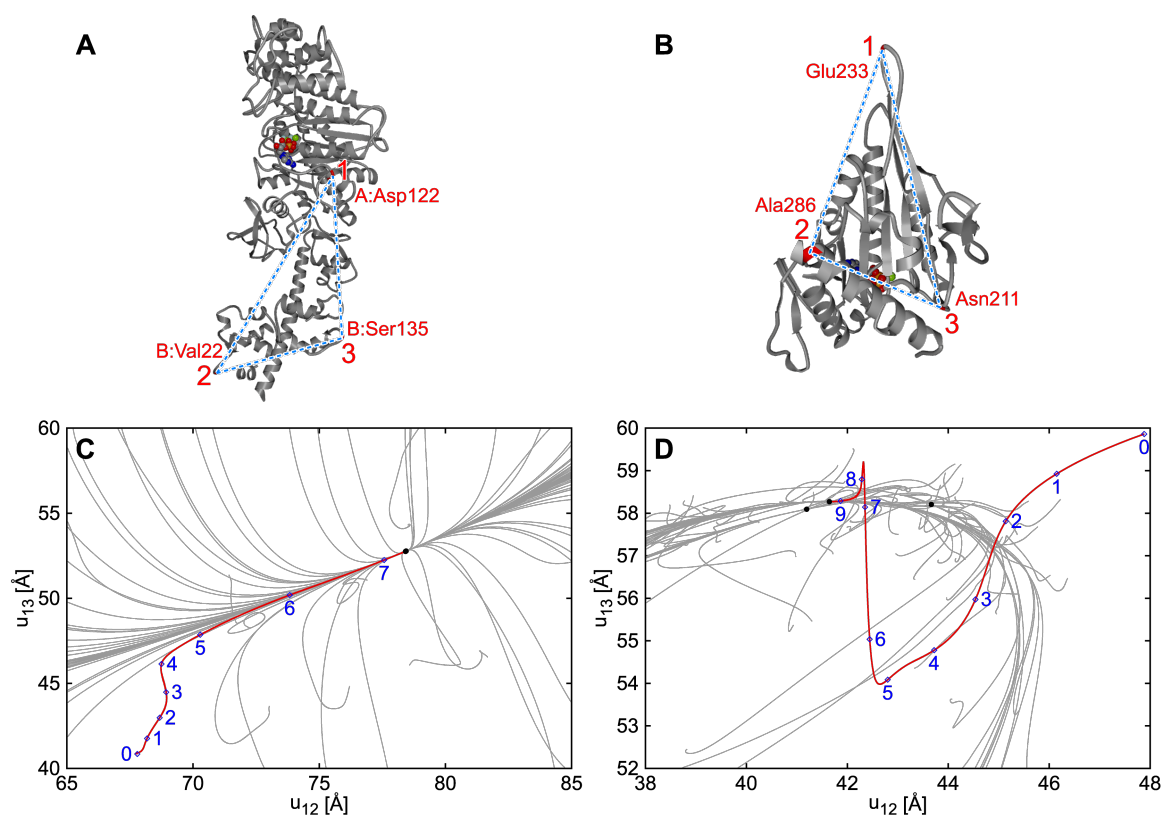
Figure 2. Relaxation paths of ENMs. Two molecular motors were compared: (**A**,**C**) Myosin V and (**B**,**D**) KIF1A; (**A**,**B**) Structure of the motors; positions of the markers 1,2,3 are shown. The ATP-bound structure of myosin V and ADP-bound structure of KIF1A were used as the reference structures to construct the ENMs; (**C**,**D**) Trajectories of conformational changes. Horizontal and vertical axes show the distances between markers 1 and 2, and markers 1 and 3, respectively. Gray lines display trajectories starting from 100 different initial deformations, prepared by applying static force toward random direction to each particle. In most cases, these trajectories quickly converge to an energetic valley (represented by a bundle of trajectories in (**C**,**D**)), and slowly return to the reference structure (stable state). This behavior is common for these two motors, and the direction of the valley around the reference structure agrees with the slowest normal mode. Red lines represent transitions between two states of the motors, which start from the nucleotide free state of myosin V (i.e., corresponding to the conformational transition upon ATP binding), and from the ATP-bound state of KIF1A (i.e., corresponding to the transition from the ATP-bound state to the ADP-bound state); label 0 shows the initial condition and the relaxation proceeded 1, 2, $\cdots$. In myosin V, the trajectory was similar to those from random deformations, and the normal mode approximation holds well except for initial changes. In KIF1A, in contrast, the relaxation progressed with multiple steps, and the trajectory converged to the slowest normal mode direction only at the final stage of relaxation (<1 Å of distance change). Reproduced from [61] with modification.

In some molecules however, we found that the region where NMA holds (i.e., the behavior is largely linear) is extremely small. In the case of KIF1A, a sequence of motion caused by steric hindrance was observed between two structural states; NMA is applicable only to the final stage of the motion. Still, the deformation of each spring was small compared to the length in the reference conformation, which supported the validity of the ENM.

3. Applications

In this way, ENMs are used for coarse-grained MD simulations, which provides information on the structural dynamics beyond NMA. Although the inherent nonlinearity may show physically interesting behavior apart from biology (e.g., glass-like, nonequilibrium behavior was observed in ENM-MD with thermal noise [63]), here we introduce examples of ENM-MD applied to more physiologically important problems.

3.1. Probing Dynamical Basis of Allostery

In these simulations using ENMs, in the same way as other models, we can apply any external forces in MD simulations (so-called steered MD simulations [64]), and also measure forces acting on any particle or spring (cf. in the linear regime, the response could be considered by ANM-NMA [65,66]). It is analogous to force probing experiments using AFM. Force-extension curves can be obtained in a similar way to AFM experiments. We can apply force (or deformation) at any part of the molecule and detect the resulting deformation or strain generated in any other parts. For example, mechanical properties of transcription activator-like effector (TALE) proteins were considered by stretching simulations [67].

As a direct application of this method, effects of external forces on molecular machines were considered. In myosin motors, it was experimentally reported that the affinity to actin filaments is modulated by the force applied to the tail (strain sensor) [68]. The actin binding domain is so far away from the tail ($\sim$10 nm) that mechanical communication between these domains is likely to exist, however the mechanism was not known. An external force was applied to the tail to mimic the experiments, and structural changes in the other parts were observed [69]. It was observed that the actin-binding interface was affected by the force. Moreover, as the computational cost is very low, we could even try applying a force to every particle (residue) in the molecule, which could systematically show the connections between the tail, actin-binding interface, and the ATP binding pocket.

This method is also applicable to study the effects of ligands, if the ligand binding can be mimicked by additional particles and springs. This approach was first developed to study the full operation cycles of hepatitis C virus helicase motor [70], which is reviewed in Section 3.2. It was also applied to actin, to study the mechanism of ATP-induced conformational changes and their effects on polymerization [71] (see Figure 3). In this work, ATP was modeled as two additional particles (ADP and P_i in Figure 3C) connected by a spring. In a slightly different way, ATP-induced conformational changes of ABC transporters were modeled and discussed [72]. As ENM-MD is effective at simulating long-time behavior, it could be used together with short all-atom MD simulations for studying structural details. A combination of targeted all-atom MD simulations and targeted ENM-MD simulations including the effect of ATP binding was adopted to investigate the inter-subunit coupling of F_1-ATPase [73].

Furthermore, this method can be applied theoretically to any kind of protein structure. The low computational cost makes it feasible to exhaustively analyze communication patterns inside the molecule for a variety of protein structures deposited in the Protein Data Bank, which may enable us to systematically study the structural basis of allosteric regulation [74].
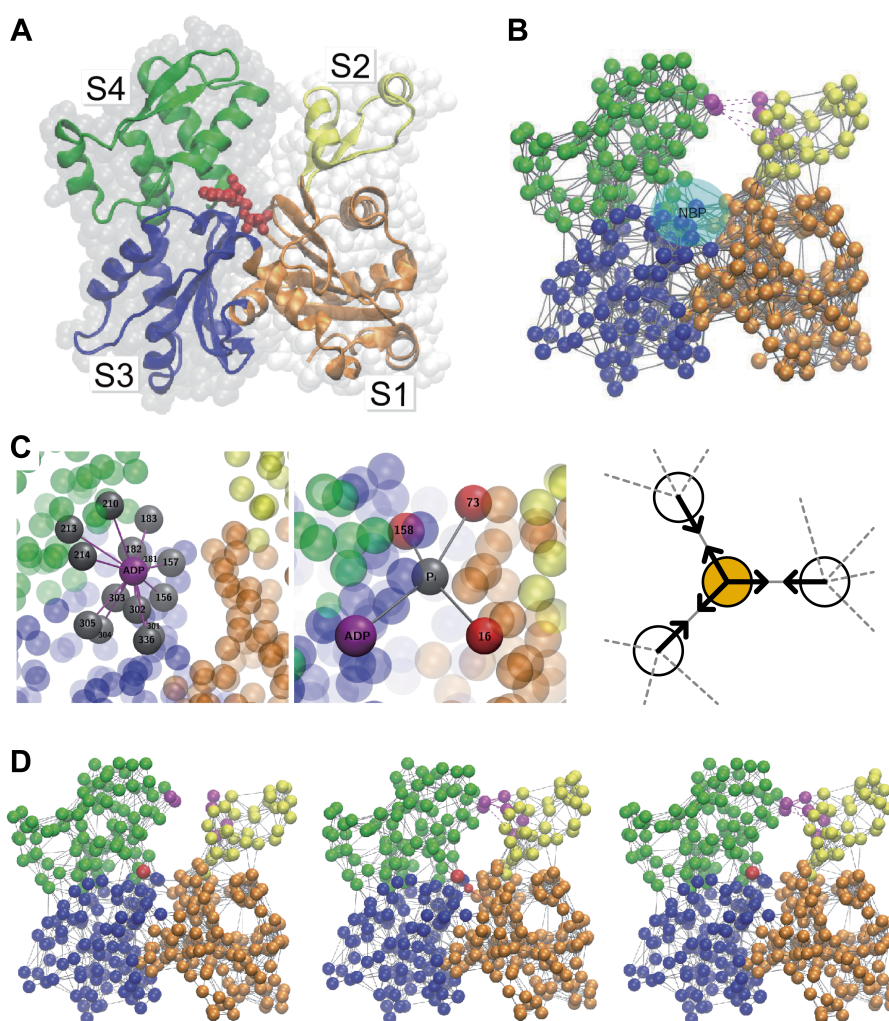
Figure 3. Ligand-induced conformational changes simulated by ENMs. (**A**) structure of G-actin and (**B**) its ENM representation; (**C**) In the nucleotide binding pocket (NBP), two additional particles (ADP and P$_i$) were introduced to mimic ligand binding. The natural lengths of springs connected to P$_i$ (solid lines in the schematic) was set shorter than the distances in the reference structure, so that they introduce attractive forces (arrows), mimicking the shrinkage of the NBP upon ATP binding; (**D**) The motion introduced by the ligand, together with additional interactions (breakable links shown in purple lines), suggested ATP-induced transition to the closed conformation (**left** to **center**), which may explain the acceleration of actin polymerization by ATP. A metastable closed state after ATP hydrolysis and P$_i$ release (**right**) was also observed. Reproduced from [71] with modification.

3.2. Tracing Entire Motor Cycles

Protein machines couple chemical events of nucleotide binding and hydrolysis to cyclic conformational motions, performed to implement a particular function. In motor proteins, such motions are used to exert forces on other proteins (such as filaments or nucleic acid strands) and produce mechanical work. Since cyclic internal motions are typically slow (with timescales ranging from milliseconds to seconds), all-atom MD simulations are not applicable despite the use of supercomputers. We used elastic networks considered as dynamical systems (beyond the NMA) to investigate the full internal operation of a motor protein.

A modeling scheme which allowed us to follow ATP-induced operation cycles in molecular machines was developed and implemented to trace the operation cycles of hepatitis C virus (HCV) helicase molecular motor (see Figure 4). Very few structures of this motor were available at that

time, and although single molecule experiments were performed, there was no consensus about the operation mechanism employed by this motor. Our elastic-network based simulations revealed the functional conformational motions which are used by this motor to translocate along single nucleic-acid strands and, at the same time, unzip duplex regions [70,75,76]. Based on these simulations we could identify the mechanism by which HCV helicase operates (see Figure 4). Our simulations could confirm the ratcheting inchworm mechanism of helicase translocation, which was previously proposed for this motor based on single-molecule experiments. The mechanism of strand separation observed from our structurally resolved simulations further supported the previously hypothesized spring-loaded unwinding mechanism.
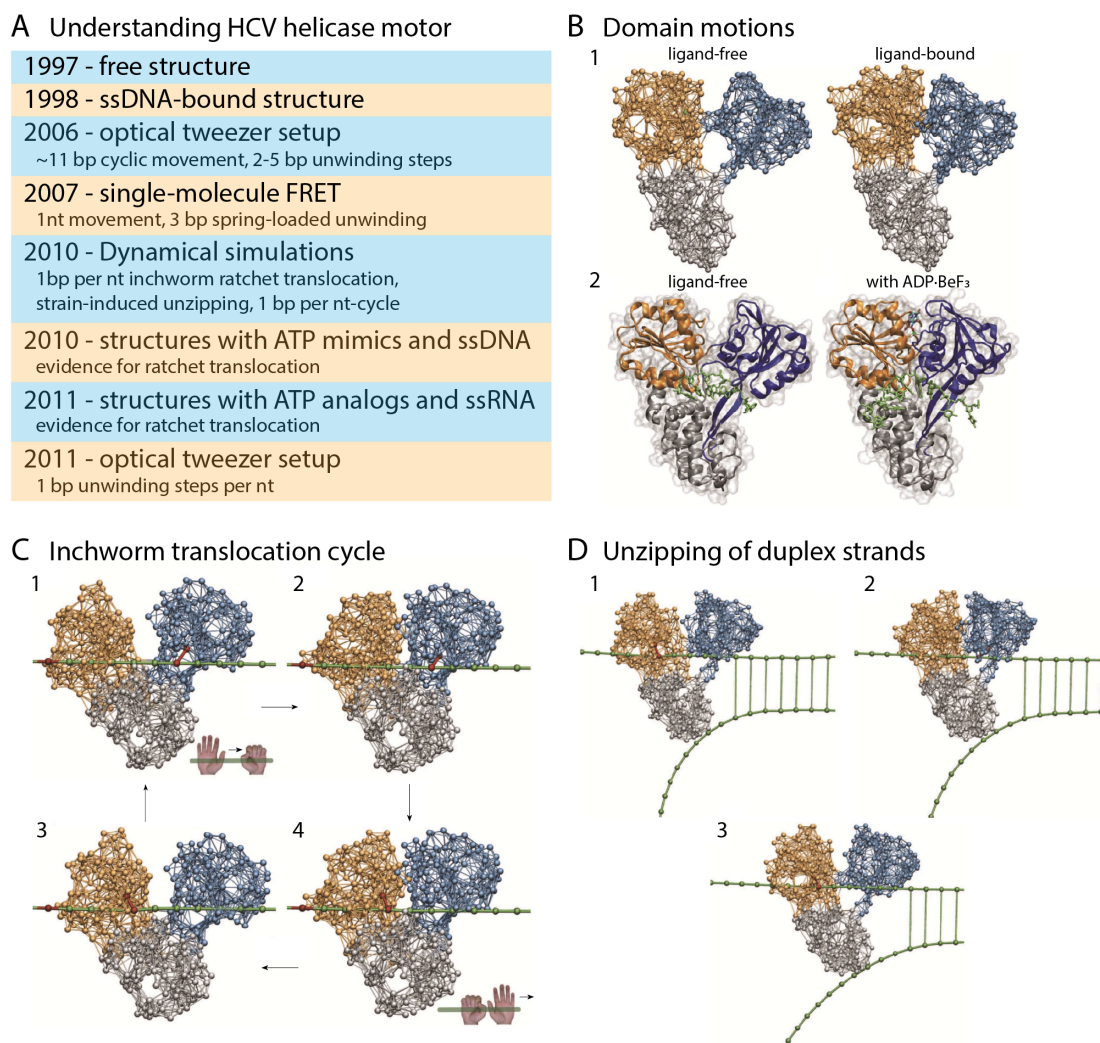
Figure 4. Entire operation cycles from ENM. (A) Table showing the main experimental efforts and observed/proposed mechanisms for the operation of the hepatitis C virus (HCV) helicase molecular motor. The references for this table are [70,77–83]; **(B–D)** Summary of results of structurally resolved dynamical simulation for HCV helicase based on ENM modeling of this motor; **(B)** Structures obtained from our simulations are compared with crystal structures from [81]; **(C)** Ratcheting inchworm translocation observed in the simulations is shown as snapshots from a single cycle. Employing the alternating hand-on hand-off mechanism of grip control on the nucleic-acid strand, the motor domains can translate their nucleotide-related internal opening and closing motion into their transport by 1 base-pair (bp) per consumed nucleotide; In **(D)**, coupling of inchworm translocation to mechanical separation of duplex strands is shown as snapshots [70,75].

After our study was reported, a variety of novel crystal structures which captured the HCV helicase motor in complex with nucleic acid substrates and together with ATP-analogs became available [81,82]. These experimental results provided further evidence for the ratcheting translocation. Furthermore, results of higher-resolution optical tweezer experiments reporting single base-pair steps of unwinding (as also seen in our coarse-grained simulations) were published [83]. Molecular simulations performed at the atomistic level provided further insights into details of the inchworm transport mechanism used by HCV helicase [84,85].

4. Further Improvement of Models and Simulation Methods

In conventional ENMs, the stiffness constant is typically the same for all springs, sometimes larger for the backbone, but not depending on the residue type or distance. In other words, all the chemical properties are omitted, unless implicitly embedded in the reference structure. It is a radical simplification, as the interactions between the sidechains depend on the type of residues; e.g., electrostatic interactions may be significant between charged residues.

Hence, efforts have been made to take into account such differences in residues in ENMs. In early days, the cutoff distance and spring constants were typically determined to maximize the correlation between the predicted intensity of fluctuations and the B-factor observed in crystallography for each residue [86]. However, this strategy relied on the crystallographic B-factor, which may not reflect the actual fluctuations in solution at room temperature. Conformational changes between two known structures were also used for the evaluation, particularly for ANMs [87]. Information on chemical bonds (e.g., hydrogen bonds between the residues) was also used to determine the parameters. To solve the cutoff dependency, a parameter-free version of ENM was also proposed [88].

Later, Dehouck and Mikhailov took another approach [89]. They extracted information on structural fluctuations from conformational ensembles obtained by NMR. Using this information, they determined the effective stiffness value, as a function of the pair of residue-types and the distance in the reference structure. As this method depends on solution NMR experiments, effects of thermal and hydrodynamic fluctuations and also hydrophobic interactions in solvent are effectively included. Besides the heterogeneous stiffness constants, a standard ENM description is employed. Hence, we can enjoy the benefits without much additional computational cost.

The construction of a protein ENM depends on the reference structure. However, although NMR and cryo-EM techniques as well as conventional crystallography have drastically evolved, high-resolution structures are not always available. ENMs could be successfully constructed from low-resolution structures [90,91], and then used for structure refinement (e.g., [92,93], followed by many others). It was also suggested that the overall shape is crucial for the determination of slow molecular motion [94]. Even further coarse-graining was possible as long as the shape was conserved [95–97] (although evaluation in these early works depended on NMA, it was suggested that slow normal modes are robust against amino-acid sequence variations [98]). This property may be beneficial when modeling a huge molecular complex such as chromatin (see Section 5).

Other than ENMs, there are many models similar to or related to ENMs. A major drawback of ENMs is that the structure cannot unfold, as the interactions are approximated by Hookean springs. When applied to multidomain proteins that can partially unfold, or include intrinsically disordered regions, breakable bonds represented by the Lennard-Jones potential are often introduced to allow unfolding. Such variants have also been used for ENM-MD simulations (e.g., [99]). This idea dates back to the 1990s (e.g., [100]), and is also related to off-lattice Gō-like models [8,9] (again, ENMs including these variants could be seen as a kind of Gō-like models, as the force field depends on a reference structure; for a perspective on MD studies using such models, see reviews e.g., [13,101]). In the examples above, to reproduce transitions between two structures, we used one structure as the reference and the other as the initial condition. This is of course a crude simplification, and smoother morphing methods have also been introduced [53–57]. Multiscale hybrid methods (e.g., all-atom MD and ANM-NMA [102]) have been developed, and combination with ENM-MD is possible.

Finally, ENMs can be combined with models of other kinds of molecules. For example, in [103], an ENM was coupled with solvent molecules represented by multiparticle collision dynamics (MPC), to consider effects of hydrodynamic fluctuations. It was shown that the conformational changes can be ordered and accelerated by hydrodynamic fluctuations (i.e., collective motion of solvent molecules). Combined with a morphing method, it was applied to adenylate kinase, which shows the relatively large open-close motion of multiple domains [104]. Again, the hydrodynamic effect alters the motion in the reaction cycles. Swimming-like behavior due to the asymmetric cyclic motion was also observed. Effects of crowding (obstacles) could be also incorporated [105]. Using MPC dynamics, substrate and/or product molecules as well as the solvent could be explicitly included into the simulation of an enzyme; e.g., enzyme kinetics of phosphoglycerate kinase was simulated [106], and reactivity of multiple active sites in 4-oxalocrotonate tautomerase was investigated [107]. External interactions such as electrostatic and van der Waals forces can also be taken into account, to study the interactions between molecules (e.g., actin and myosin [108]).

5. Discussion

To summarize, ENMs are of wide use not only for analysis of structural fluctuations using NMA but also for reproducing dynamic processes using molecular dynamics, and even entire machine operation cycles.

The dynamic properties of proteins were compared with those of random or designed artificial elastic networks [60]. It was later reported that ENMs constructed for fractal polymer globules also showed relaxation dynamics similar to that of protein ENMs [109]. Furthermore, designed elastic network structures that reproduce "protein-like" features can be considered and compared with ENMs of real proteins. For example, machine-like motions induced by ligand binding were demonstrated [60], and models of linear motors were constructed [110,111]. ENMs mimicking allosteric effects could be constructed through evolutionary optimization of the structure [112]. Although it is beyond the scope of this review, we hope this direction of study will help to elucidate the design principles of protein structures, independent of the history of evolution. For a discussion of those aspects, we refer the reader to [113].

Recently, ENMs have also been used for biomolecules other than proteins. Complexes of proteins and nucleic acids such as ribosomes [114] and nucleosomes [115] were modeled as ENMs, and their dynamics were analyzed by NMA. Structures of free DNA double-strands were predicted from their sequences and modeled as ANMs (at different coarse-graining levels where each particle represents an atom to several bases), and their structural fluctuations were analyzed by NMA [116,117]. Furthermore, GNM was applied to chromatin structure (DNA-protein complex in the cell nucleus) [118]. Each particle corresponds to kilobases of DNA, which is much larger than an amino acid residue in proteins. Despite the difference in resolution, the mobility of genomic loci was successfully predicted by NMA in a similar way as for proteins. In this particular case, GNM has an advantage that it could be constructed from only the neighbor matrix obtained by Hi-C experiments; nonetheless, with 3D structure reconstruction, ANM-type models can also be constructed from the experimental data, which can also be readily used for dynamic simulations and will provide more information on the structural fluctuations.

Using all-atom MD simulations is still challenging and needs specialized hardware to exceed milliseconds even for a small protein [4,119]. In high-performance computing (HPC) using massively parallel supercomputers, it is generally much harder to utilize the parallelism for solving the same size of problem faster (strong scaling) than solving a larger problem within the same time (weak scaling). Assuming the same computational effort and lapse-time, the former represents simulations of long-time behavior of a small protein, while the latter corresponds to simulations of a huge complex for a short period. Considering the current trend of HPC depending on huge parallelism, such low-cost methods using ENMs and other simplified models will remain useful, serving as a realistic and convenient choice in the future.

Appendix A. Mathematical Representation of the Models

Appendix A.1. Elastic Network Models

As introduced in Section 2.1, ENMs consist of point-like particles connected by springs. To construct an ENM for a protein, a structural data set (typically chosen from the Protein Data Bank) is used as the reference. In the simplest form, coarse-grained ENMs are constructed and mathematically represented as follows (see also Figure 1).
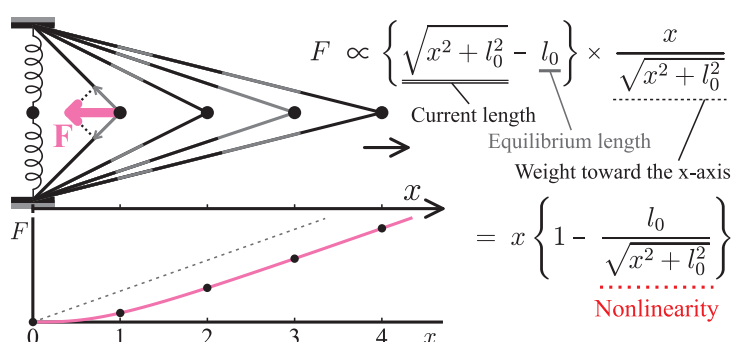
Figure A1. An illustrative example of the nonlinearity. Two springs are initially aligned straight without strains; each spring obeys Hooke's law (equilibrium length: l_0). If we pull the midpoint perpendicularly to the initial spring direction, the strength F of the resultant force **F** depends nonlinearly on the displacement x. Adapted from [62].

The coordinate of each α-carbon atom in the reference structure is used as the equilibrium position $\mathbf{R}_i^{(0)}$ of the corresponding network particle. For each pair of particles, if the distance $d_{ij}^{(0)} = \left| \mathbf{R}_i^{(0)} - \mathbf{R}_j^{(0)} \right|$ in the reference structure is less than the cutoff distance l_0, the pair is connected by a spring; the equilibrium length of the spring is equal to $d_{ij}^{(0)}$, i.e., springs are not strained in the reference conformation. All the springs have the same stiffness constant κ.

Each spring obeys Hooke's law. The force direction coincides with the spring direction (without torsion). Then, the spring that connects particles i and j exerts force

$$\mathbf{F}_{ij} = -\kappa \left(d_{ij} - d_{ij}^{(0)} \right) \frac{\mathbf{R}_i - \mathbf{R}_j}{d_{ij}} \tag{A1}$$

on particle i. Here, $\mathbf{R}_i$ is the current coordinate of particle i, and $d_{ij} = \left| \mathbf{R}_i - \mathbf{R}_j \right|$ is the actual distance between particles i and j. Thus, the resultant force acting on particle i is

$$\mathbf{F}_i = -\kappa \sum_{j=1}^{N} A_{ij} \left(d_{ij} - d_{ij}^{(0)} \right) \frac{\mathbf{R}_i - \mathbf{R}_j}{d_{ij}}, \tag{A2}$$

where N is the number of particles in the network, and the adjacency matrix $A_{ij} = 1$ if $d_{ij}^{(0)} < l_0$ and $A_{ij} = 0$ otherwise. It should be noted that, although the forces (A2) are linear in terms of changes in

the spring lengths, they are still nonlinear because distance d_{ij} has nonlinear dependence on the spatial coordinates, i.e., $d_{ij} = \sqrt{(x_i - x_j)^2 + (y_i - y_j)^2 + (z_i - z_j)^2}$. The total elastic energy of the network is

$$U = \frac{\kappa}{2} \sum_{i<j} A_{ij} \left(d_{ij} - d_{ij}^{(0)} \right)^2. \tag{A3}$$

In ENM-MD simulations (Section 2.4), Newton's equations of motion with the forces represented by Equation (A2) are numerically solved. When we consider slow conformational dynamics of proteins in the solvent, the motion is assumed to be overdamped [23]. We also ignore hydrodynamic effects (cf. combination with MPC solvent [103]). Then, in the overdamped limit (i.e., the velocity of each particle is proportional to the total force acting on it), the motion of particle i (at time t) is governed by

$$\frac{d\mathbf{R}_i}{dt} = \Gamma_i \mathbf{F}_i, \tag{A4}$$

where Γ_i is the mobility. Here, we assume the same mobility for all the particles, i.e., $\Gamma_i = \Gamma$. With rescaling of time (measured in units of $(\Gamma\kappa)^{-1}$), the dynamics are explicitly represented by

$$\frac{d\mathbf{R}_i}{dt} = -\sum_{j=1}^{N} A_{ij} \left(\left| \mathbf{R}_i - \mathbf{R}_j \right| - \left| \mathbf{R}_i^{(0)} - \mathbf{R}_j^{(0)} \right| \right) \frac{\mathbf{R}_i - \mathbf{R}_j}{\left| \mathbf{R}_i - \mathbf{R}_j \right|}. \tag{A5}$$

Figure 2 shows relaxation dynamics simulated in this way [61]. Random initial deformations (for gray lines) were prepared by simulations under additional static forces, starting from the reference conformation. Specifically, random static forces $\mathbf{f}_i$ acting on particle i were independently generated with the constraint such that $\sum_i |\mathbf{f}_i|^2$ is constant (designated force intensity), and then

$$\frac{d\mathbf{R}_i}{dt} = \mathbf{f}_i - \sum_{j=1}^{N} A_{ij} \left(\left| \mathbf{R}_i - \mathbf{R}_j \right| - \left| \mathbf{R}_i^{(0)} - \mathbf{R}_j^{(0)} \right| \right) \frac{\mathbf{R}_i - \mathbf{R}_j}{\left| \mathbf{R}_i - \mathbf{R}_j \right|}. \tag{A6}$$

was used instead of Equation (A5). After a certain length of simulation, the final conformation was in turn used as the initial condition for the relaxation simulation.

Appendix A.2. Normal Mode Analysis

NMA is often adopted for ENMs (Section 2.2). In NMA, the motion is linearly approximated around the steady state, and then decomposed into normal modes. The forces are linearly approximated in terms of displacements, and represented by using a linearization matrix. For conservative forces, it is equal to the Hessian matrix of the potential energy. Each eigenvalue of the matrix shows the frequency (in underdamped cases) or decay rate (in the overdamped limit) of the motion toward the direction of the corresponding eigenvector.

When NMA is applied to GNMs with uniform stiffness and mass (mobility), we can simply use the Kirchhoff matrix (connectivity matrix). For ANMs, we provide a brief explanation below.

If deviation $\Delta \mathbf{R}_i = \mathbf{R}_i - \mathbf{R}_i^{(0)}$ from the reference conformation is sufficiently small for all the particles, Equation (A5) can be linearized as

$$\frac{d}{dt} \Delta \mathbf{R}_i = -\sum_{j=1}^{N} A_{ij} \left[\mathbf{u}_{ij}^{(0)} \cdot \left(\Delta \mathbf{R}_i - \Delta \mathbf{R}_j \right) \right] \mathbf{u}_{ij}^{(0)}, \tag{A7}$$

where $\mathbf{u}_{ij}^{(0)} = \left(\mathbf{R}_i^{(0)} - \mathbf{R}_j^{(0)} \right) / d_{ij}^{(0)}$; i.e., the change in spring length can be linearly approximated as the inner product of the unit vector $\mathbf{u}_{ij}^{(0)}$ toward the spring direction in the reference conformation and the relative displacement vector $\left(\Delta \mathbf{R}_i - \Delta \mathbf{R}_j \right)$ (see Figure 1). It is worthwhile to compare the linearized

forces in Equation (A7) which have static directions $\mathbf{u}_{ij}^{(0)}$, with the exact forces in Equation (A5) which act along the actual orientations of the springs.

The set of linearized Equation (A7) should be a good approximation as long as the deviations (changes in the Cartesian coordinates) $\mathbf{\Delta R}_i$ are much smaller than the equilibrium lengths $d_{ij}^{(0)}$ of springs between particles. Therefore, by comparing the coordinate changes with the typical equilibrium lengths, we can formulate an estimate for the validity of the approximation. In a typical protein ENM with cutoff distance 10 Å, we can assume (as a rough estimate) a value of 5 Å for the average equilibrium length of springs. Then, the linear description should hold for coordinate changes much smaller than that value, i.e., they should not be larger than, e.g., 10% of it (0.5 Å).

Equation (A7) is represented in the matrix form

$$\frac{d}{dt}\mathbf{\Delta R}_i = -\sum_{j=1}^{N} \mathbf{\Lambda}_{ij}\mathbf{\Delta R}_j. \tag{A8}$$

$\mathbf{\Lambda}$ is a $3N \times 3N$ matrix:

$$\Lambda_{i\sigma,j\eta} = A_{ij}u_{ij,\sigma}^{(0)}u_{ij,\eta}^{(0)} \text{ (for } i \neq j\text{)}, \quad \Lambda_{i\sigma,i\eta} = -\sum_{j} A_{ij}u_{ij,\sigma}^{(0)}u_{ij,\eta}^{(0)}; \tag{A9}$$

where σ, $\eta \in \{x, y, z\}$. Note that this result is equivalent to the Hessian matrix of the potential U in Equation (A3) with rescaling.

The general solution of Equation (A8) is given as the superposition of $3N - 6$ exponentially decaying normal modes, i.e.,

$$\mathbf{\Delta R}_i(t) = \sum_{\alpha=1}^{3N-6} k_\alpha e^{-\lambda_\alpha t}\mathbf{e}_i^{(\alpha)}, \tag{A10}$$

where λ_α are the eigenvalues, and $\mathbf{e}_i^{(\alpha)}$ are the corresponding eigenvectors, of matrix $\mathbf{\Lambda}$. Each eigenvalue λ_α represents the decay rate of the normal mode (cf. in the underdamped case, λ_α represents the vibrational frequency).

Matrix $\mathbf{\Lambda}$ has $3N$ eigenvalues, however 6 of them are always zero, corresponding to the global translation and rotation. Note that instead of Cartesian coordinates, internal coordinates such as dihedral angles can be chosen as variables [42,44,120,121], which dates back to early works e.g., [24]. At the cost of simplicity of the potential function and its Hessian, the degree of freedom could be drastically reduced; that is beneficial for large models for which the computational cost for the eigenvalue problem (matrix diagonalization) is huge.

References

1.　Ando, T.; Uchihashi, T.; Scheuring, S. Filming biomolecular processes by high-speed atomic force microscopy. *Chem. Rev.* **2014**, *114*, 3120–3188. [CrossRef] [PubMed]
2.　Ando, T. Directly watching biomolecules in action by high-speed atomic force microscopy. *Biophys. Rev.* **2017**, *9*, 421–429. [CrossRef] [PubMed]
3.　McCammon, J.A.; Gelin, B.R.; Karplus, M. Dynamics of folded proteins. *Nature* **1977**, *267*, 585–590. [CrossRef]
4.　Shaw, D.E.; Dror, R.O.; Salmon, J.K.; Grossman, J.P.; Mackenzie, K.M.; Bank, J.A.; Young, C.; Deneroff, M.M.; Batson, B.; Bowers, K.J.; et al. Millisecond-scale molecular dynamics simulations on Anton. In Proceedings of the Conference on High Performance Computing, Networking, Storage and Analysis (SC09), Portland, OR, USA, 14–20 November 2009.
5.　Yu, I.; Mori, T.; Ando, T.; Harada, R.; Jung, J.; Sugita, Y.; Feig, M. Biomolecular interactions modulate macromolecular structure and dynamics in atomistic model of a bacterial cytoplasm. *eLife* **2016**, *5*, e19274. [CrossRef] [PubMed]
6.　Perilla, J.R.; Hadden, J.A.; Goh, B.C.; Mayne, C.G.; Schulten, K. All-atom molecular dynamics of virus capsids as drug targets. *J. Phys. Chem. Lett.* **2016**, *7*, 1836–1844. [CrossRef] [PubMed]

7. Marrink, S.J.; Tieleman, D.P. Perspective on the Martini model. *Chem. Soc. Rev.* **2013**, *42*, 6801–6822. [CrossRef] [PubMed]

8. Gō, N. Theoretical studies of protein folding. *Ann. Rev. Biophys. Bioeng.* **1983**, *12*, 183–210. [CrossRef] [PubMed]

9. Clementi, C.; Nymeyer, H.; Onuchic, J.N. Topological and energetic factors: What determines the structural details of the transition state ensemble and "en-route" intermediates for protein folding? An investigation for small globular proteins. *J. Mol. Biol.* **2000**, *298*, 937–953. [CrossRef] [PubMed]

10. Kenzaki, H.; Koga, N.; Hori, N.; Kanada, R.; Li, W.; Okazaki, K.; Yao, X.-Q.; Takada, S. CafeMol: A coarse-grained biomolecular simulator for simulating proteins at work. *J. Chem. Theory Comput.* **2011**, *7*, 1979–1989. [CrossRef] [PubMed]

11. Li, W.; Wolynes, P.G.; Takada, S. Frustration, specific sequence dependence, and nonlinearity in large-amplitude fluctuations of allosteric proteins. *Proc. Natl. Acad. Sci. USA* **2011**, *108*, 3504–3509. [CrossRef] [PubMed]

12. Li, W.; Wang, W.; Takada, S. Energy landscape views for interplays among folding, binding, and allostery of calmodulin domains. *Proc. Natl. Acad. Sci. USA* **2014**, *111*, 10550–10555. [CrossRef] [PubMed]

13. Takada, S. Coarse-grained molecular simulations of large biomolecules. *Curr. Opin. Struct. Biol.* **2012**, *22*, 130–137. [CrossRef] [PubMed]

14. Tirion, M.M. Large amplitude elastic motions in proteins from a single-parameter, atomic analysis. *Phys. Rev. Lett.* **1996**, *77*, 1905–1908. [CrossRef] [PubMed]

15. Hinsen, K. Analysis of domain motions by approximate normal mode calculations. *Proteins* **1998**, *33*, 417–429. [CrossRef]

16. Bahar, I.; Atilgan, A.R.; Erman, B. Direct evaluation of thermal fluctuations in proteins using a single-parameter harmonic potential. *Fold. Des.* **1997**, *2*, 173–181. [CrossRef]

17. Haliloglu, T.; Bahar, I.; Erman, B. Gaussian dynamics of folded proteins. *Phys. Rev. Lett.* **1997**, *79*, 3090–3093. [CrossRef]

18. Atilgan, C.; Gerek, Z.N.; Ozkan, S.B.; Atilgan, A.R. Manipulation of conformational change in proteins by single-residue perturbations. *Biophys. J.* **2010**, *99*, 933–943. [CrossRef] [PubMed]

19. James, H.M.; Guth, E. Theory of the increase in rigidity of rubber during cure. *J. Chem. Phys.* **1947**, *15*, 669–683. [CrossRef]

20. Flory, P.J. Statistical thermodynamics of random networks. *Proc. R. Soc. A* **1976**, *351*, 351–380. [CrossRef]

21. Doruker, P.; Atilgan, A.R.; Bahar, I. Dynamics of proteins predicted by molecular dynamics simulations and analytical approaches: Application to α-amylase inhibitor. *Proteins* **2000**, *40*, 512–524. [CrossRef]

22. Atilgan, A.R.; Durell, S.R.; Jernigan, R.L.; Demirel, M.C.; Keskin, O.; Bahar, I. Anisotropy of Fluctuation Dynamics of Proteins with an Elastic Network Model. *Biophys. J.* **2001**, *80*, 505–515. [CrossRef]

23. Kitao, A.; Hirata, F.; Gō, N. The effects of solvent on the conformation and the collective motions of protein: Normal mode analysis and molecular dynamics simulations of melittin in water and in vacuum. *Chem. Phys.* **1991**, *158*, 447–472. [CrossRef]

24. Gō, N.; Noguti, T.; Nishikawa, T. Dynamics of a small globular protein in terms of low-frequency vibrational modes. *Proc. Natl. Acad. Sci. USA* **1983**, *80*, 3696–3700. [CrossRef] [PubMed]

25. Brooks, B.; Karplus, M. Harmonic dynamics of proteins: Normal modes and fluctuations in bovine pancreatic trypsin inhibitor. *Proc. Natl. Acad. Sci. USA* **1983**, *80*, 6571–6575. [CrossRef] [PubMed]

26. Levy, R.M.; Srinivasan, A.R.; Olson, W.K.; McCammon, J.A. Quasi-harmonic method for studying very low frequency modes in proteins. *Biopolymers* **1984**, *23*, 1099–1112. [CrossRef] [PubMed]

27. Brooks, B.; Karplus, M. Normal modes for specific motions of macromolecules: Application to the hinge-bending mode of lysozyme. *Proc. Natl. Acad. Sci. USA* **1985**, *82*, 4995–4999. [CrossRef] [PubMed]

28. Levitt, M.; Sander, C.; Stern, P.S. Protein normal-mode dynamics: Trypsin inhibitor, crambin, ribonuclease and lysozyme. *J. Mol. Biol.* **1985**, *181*, 423–447. [CrossRef]

29. Yang, L.-W.; Bahar, I. Coupling between catalytic site and collective dynamics: A requirement for mechanochemical activity of enzymes. *Structure* **2005**, *13*, 893–904. [CrossRef]

30. Liao, J.-L.; Beratan, D.N. How does protein architecture facilitate the transduction of ATP chemical-bond energy into mechanical work? The cases of nitrogenase and ATP binding-cassette proteins. *Biophys. J.* **2004**, *87*, 1369–1377. [CrossRef]

31. Chennubhotla, C.; Rader, A.J.; Yang, L.-W.; Bahar, I. Elastic network models for understanding biomolecular machinery: From enzymes to supramolecular assemblies. *Phys. Biol.* **2005**, *2*, S173–S180. [CrossRef]

32. Shrivastava, I.H.; Bahar, I. Common mechanism of pore opening shared by five different potassium channels. *Biophys. J.* **2006**, *90*, 3929–3940. [CrossRef] [PubMed]

33. Tama, F.; Sanejouand, Y.-H. Conformational change of proteins arising from normal mode calculations. *Protein Eng.* **2001**, *14*, 1–6. [CrossRef] [PubMed]

34. Zheng, W.; Doniach, S. A comparative study of motor-protein motions by using a simple elastic-network model. *Proc. Natl. Acad. Sci. USA* **2003**, *100*, 13253–13258. [CrossRef] [PubMed]

35. Anisotropic Network Model Web Server 2.1. Available online: http://anm.csb.pitt.edu/ (accessed on 5 December 2018).

36. Eyal, E.; Lum, G.; Bahar, I. The anisotropic network model web server at 2015 (ANM 2.0). *Bioinformatics* **2015**, *31*, 1487–1489. [CrossRef] [PubMed]

37. DynOmics Using Elastic Network Models—ENM 1.0. Available online: http://enm.pitt.edu/ (accessed on 5 December 2018).

38. Li, H.; Chang, Y.-Y.; Lee, J.Y.; Bahar, I.; Yang, L.-W. DynOmics: Dynamics of structural proteome and beyond. *Nucleic Acids Res.* **2017**, *45*, W374–W380. [PubMed]

39. iGNM 2.0—Gaussian Network Model Database. Available online: http://gnmdb.csb.pitt.edu/ (accessed on 5 December 2018).

40. Li, H.; Chang, Y.-Y.; Yang, L.-W.; Bahar, I. iGNM 2.0: The Gaussian network model database for biomolecular structural dynamics. *Nucleic Acids Res.* **2016**, *44*, D415–D422. [CrossRef]

41. iMODS. Available online: http://imods.chaconlab.org/ (accessed on 5 December 2018).

42. López-Blanco, J.R.; Aliaga, J.I.; Quintana-Ortí, E.S.; Chacón, P. iMODS: Internal coordinates normal mode analysis server. *Nucleic Acids Res.* **2014**, *42*, W271–W276. [CrossRef] [PubMed]

43. Promode Elastic. Available online: https://pdbj.org/promode-elastic (accessed on 5 December 2018).

44. Wako, H.; Endo, S. Normal mode analysis as a method to derive protein dynamics information from the Protein Data Bank. *Biophys. Rev.* **2017**, *9*, 877–893. [CrossRef]

45. Ma, J. Usefulness and limitations of normal mode analysis in modeling dynamics of biomolecular complexes. *Structure* **2005**, *13*, 373–380. [CrossRef]

46. Bahar, I.; Rader, A.J. Coarse-grained normal mode analysis in structural biology. *Curr. Opin. Struct. Biol.* **2005**, *15*, 586–592. [CrossRef]

47. Cui, Q.; Bahar, I. (Eds.) *Normal Mode Analysis: Theory and Applications to Biological and Chemical Systems*; Chapman and Hall/CRC: Boca Raton, FL, USA, 2006.

48. Tama, F.; Brooks, C.L., III. Symmetry, form, and shape: Guiding principles for robustness in macromolecular machines. *Annu. Rev. Biophys. Biomol. Struct.* **2006**, *35*, 115–133. [CrossRef] [PubMed]

49. Bahar, I.; Lezon, T.R.; Yang, L.-W.; Eyal, E. Global dynamics of proteins: Bridging between structure and function. *Annu. Rev. Biophys.* **2010**, *39*, 23–42. [CrossRef] [PubMed]

50. Bahar, I.; Cheng, M.H.; Lee, J.Y.; Kaya, C.; Zhang, S. Structure-encoded global motions and their role in mediating protein-substrate interactions. *Biophys. J.* **2015**, *109*, 1101–1109. [CrossRef] [PubMed]

51. López-Blanco, J.R.; Chacón, P. New generation of elastic network models. *Curr. Opin. Struct. Biol.* **2016**, *37*, 46–53. [CrossRef] [PubMed]

52. Miyashita, O.; Onuchic, J.N.; Wolynes, P.G. Nonlinear elasticity, proteinquakes, and the energy landscapes of functional transitions in proteins. *Proc. Natl. Acad. Sci. USA* **2003**, *100*, 12570–12575. [CrossRef] [PubMed]

53. Kim, M.K.; Chirikjian, G.S.; Jernigan, R.L. Elastic models of conformational transitions in macromolecules. *J. Mol. Graph. Model.* **2002**, *21*, 151–160. [CrossRef]

54. Maragakis, P.; Karplus, M. Large amplitude conformational change in proteins explored with a plastic network model: Adenylate kinase. *J. Mol. Biol.* **2005**, *352*, 807–822. [CrossRef] [PubMed]

55. Zheng, W.; Brooks, B.R.; Hummer, G. Protein conformational transitions explored by mixed elastic network models. *Proteins* **2007**, *69*, 43–57. [CrossRef]

56. Tekpinar, M.; Zheng, W. Predicting order of conformational changes during protein conformational transitions using an interpolated elastic network model. *Proteins* **2010**, *78*, 2469–2481. [CrossRef]

57. Lee, B.H.; Seo, S.; Kim, M.H.; Kim, Y.; Jo, S.; Choi, M.; Lee, H.; Choi, J.B.; Kim, M.K. Normal mode-guided transition pathway generation in proteins. *PLoS ONE* **2017**, *12*, e0185658. [CrossRef]

58. Juanico, B.; Sanejouand, Y.-H.; Piazza, F.; De Los Rios, P. Discrete breathers in nonlinear network models of proteins. *Phys. Rev. Lett.* **2007**, *99*, 238104. [CrossRef] [PubMed]

59. Morgan, S.E.; Cole, D.J.; Chin, A.W. Nonlinear network model analysis of vibrational energy transfer and localisation in the Fenna-Matthews-Olson complex. *Sci. Rep.* **2016**, *6*, 36703. [CrossRef] [PubMed]

60. Togashi, Y.; Mikhailov, A.S. Nonlinear relaxation dynamics in elastic networks and design principles of molecular machines. *Proc. Natl. Acad. Sci. USA* **2007**, *104*, 8697–8702. [CrossRef]

61. Togashi, Y.; Yanagida, T.; Mikhailov, A.S. Nonlinearity of mechanochemical motions in motor proteins. *PLoS Comput. Biol.* **2010**, *6*, e1000814. [CrossRef] [PubMed]

62. Togashi, Y. Dynamical features and design principles of protein machines: Elastic network studies. *Seibutsu Butsuri* **2008**, *48*, 114–118. [CrossRef]

63. Hayashi, K.; Takano, M. Violation of the fluctuation-dissipation theorem in a protein system. *Biophys. J.* **2007**, *93*, 895–901. [CrossRef] [PubMed]

64. Izrailev, S.; Stepaniants, S.; Balsera, M.; Oono, Y.; Schulten, K. Molecular dynamics study of unbinding of the avidin-biotin complex. *Biophys. J.* **1997**, *72*, 1568–1581. [CrossRef]

65. Eyal, E.; Bahar, I. Toward a molecular understanding of the anisotropic response of proteins to external forces: Insights from elastic network models. *Biophys. J.* **2008**, *94*, 3424–3435. [CrossRef]

66. Yang, L.-W.; Kitao, A.; Huang, B.-C.; Gō, N. Ligand-induced protein responses and mechanical signal propagation described by linear response theories. *Biophys. J.* **2014**, *107*, 1415–1425. [CrossRef]

67. Flechsig, H. TALEs from a spring—Superelasticity of Tal effector protein structures. *PLoS ONE* **2014**, *9*, e109919. [CrossRef]

68. Iwaki, M.; Iwane, A.H.; Shimokawa, T.; Cooke, R.; Yanagida, T. Brownian search-and-catch mechanism for myosin-VI steps. *Nat. Chem. Biol.* **2009**, *5*, 403–405. [CrossRef] [PubMed]

69. Düttmann, M.; Togashi, Y.; Yanagida, T.; Mikhailov, A.S. Myosin-V as a mechanical sensor: An elastic network study. *Biophys. J.* **2012**, *102*, 542–551. [CrossRef] [PubMed]

70. Flechsig, H.; Mikhailov, A.S. Tracing entire operation cycles of molecular motor hepatitis C virus helicase in structurally resolved dynamical simulations. *Proc. Natl. Acad. Sci. USA* **2010**, *107*, 20875–20880. [CrossRef] [PubMed]

71. Düttmann, M.; Mittnenzweig, M.; Togashi, Y.; Yanagida, T.; Mikhailov, A.S. Complex intramolecular mechanics of G-actin—An elastic network study. *PLoS ONE* **2012**, *7*, e45859. [CrossRef] [PubMed]

72. Flechsig, H. Nucleotide-induced conformational dynamics in ABC transporters from structure-based coarse grained modeling. *Front. Phys.* **2016**, *4*, 3. [CrossRef]

73. Dai, L.; Flechsig, H.; Yu, J. Deciphering intrinsic inter-subunit couplings that lead to sequential hydrolysis of F$_1$-ATPase ring. *Biophys. J.* **2017**, *113*, 1440–1453. [CrossRef] [PubMed]

74. Togashi, Y. Screening for mechanical responses of proteins using coarse-grained elastic network models. *NOLTA IEICE* **2016**, *7*, 190–201. [CrossRef]

75. Flechsig, H. Computational biology approach to uncover hepatitis C virus helicase operation. *World J. Gastroenterol.* **2014**, *20*, 3401–3409. [CrossRef]

76. Flechsig, H.; Popp, D.; Mikhailov, A.S. *In silico* investigation of conformational motions in superfamily 2 helicase proteins. *PLoS ONE* **2011**, *6*, e21809. [CrossRef]

77. Yao, N.; Hesson, M.; Cable, M.; Hong, Z.; Kwong, A.D.; Le, H.V.; Weber, P.C. Structure of the hepatitis C virus RNA helicase domain. *Nat. Struct. Biol.* **1997**, *4*, 463–467. [CrossRef]

78. Kim, J.L.; Morgenstern, K.A.; Griffith, J.P.; Dwyer, M.D.; Thomson, J.A.; Murcko, M.A.; Lin, C.; Caron, P.R. Hepatitis C virus NS3 RNA helicase domain with a bound oligonucleotide: The crystal structure provides insights into the mode of unwinding. *Structure* **1998**, *6*, 89–100. [CrossRef]

79. Dumont, S.; Cheng, W.; Serebrov, V.; Beran, R.K.; Tinoco, I., Jr.; Pyle, A.M.; Bustamante, C. RNA translocation and unwinding mechanism of HCV NS3 helicase and its coordination by ATP. *Nature* **2006**, *439*, 105–108. [CrossRef] [PubMed]

80. Myong, S.; Bruno, M.M.; Pyle, A.M.; Ha, T. Spring-loaded mechanism of DNA unwinding by hepatitis C virus NS3 helicase. *Science* **2007**, *317*, 513–516. [CrossRef] [PubMed]

81. Gu, M.; Rice, C.M. Three conformational snapshots of the hepatitis C virus NS3 helicase reveal a ratchet translocation mechanism. *Proc. Natl. Acad. Sci. USA* **2010**, *107*, 521–528. [CrossRef] [PubMed]

82. Appleby, T.C.; Anderson, R.; Fedorova, O.; Pyle, A.M.; Wang, R.; Liu, X.; Brendza, K.M.; Somoza, J.R. Visualizing ATP-dependent RNA translocation by the NS3 helicase from HCV. *J. Mol. Biol.* **2011**, *405*, 1139–1153. [CrossRef] [PubMed]

83. Cheng, W.; Arunajadai, S.G.; Moffitt, J.R.; Tinoco, I., Jr.; Bustamante, C. Single-base pair unwinding and asynchronous RNA release by the hepatitis C virus NS3 helicase. *Nature* **2011**, *333*, 1746–1749.

84. Zheng, W.; Tekpinar, M. Structure-based simulations of the translocation mechanism of the hepatitis C virus NS3 helicase along single-stranded nucleic acid. *Biophys. J.* **2012**, *103*, 1343–1353. [CrossRef] [PubMed]

85. Pérez-Villa, A.; Darvas, M.; Bussi, G. ATP dependent NS3 helicase interaction with RNA: Insights from molecular simulations. *Nucleic Acids Res.* **2015**, *43*, 8725–8734. [CrossRef]

86. Kondrashov, D.A.; Cui, Q.; Phillips, G.N., Jr. Optimization and evaluation of a coarse-grained model of protein motion using X-ray crystal data. *Biophys. J.* **2006**, *91*, 2760–2767. [CrossRef]

87. Jeong, J.I.; Jang, Y.; Kim, M.K. A connection rule for *α*-carbon coarse-grained elastic network models using chemical bond information. *J. Mol. Graph. Model.* **2006**, *24*, 296–306. [CrossRef]

88. Yang, L.; Song, G.; Jernigan, R.L. Protein elastic network models and the ranges of cooperativity. *Proc. Natl. Acad. Sci. USA* **2009**, *106*, 12347–12352. [CrossRef] [PubMed]

89. Dehouck, Y.; Mikhailov, A.S. Effective harmonic potentials: Insights into the internal cooperativity and sequence-specificity of protein dynamics. *PLoS Comput. Biol.* **2013**, *9*, e1003209. [CrossRef] [PubMed]

90. Tama, F.; Wriggers, W.; Brooks, C.L., III. Exploring global distortions of biological macromolecules and assemblies from low-resolution structural information and elastic network theory. *J. Mol. Biol.* **2002**, *321*, 297–305. [CrossRef]

91. Ming, D.; Kong, Y.; Lambert, M.A.; Huang, Z.; Ma, J. How to describe protein motion without amino acid sequence and atomic coordinates. *Proc. Natl. Acad. Sci. USA* **2002**, *99*, 8620–8625. [CrossRef] [PubMed]

92. Tama, F.; Miyashita, O.; Brooks, C.L., III. Flexible multi-scale fitting of atomic structures into low-resolution electron density maps with elastic network normal mode analysis. *J. Mol. Biol.* **2004**, *337*, 985–999. [CrossRef] [PubMed]

93. Delarue, M.; Dumas, P. On the use of low-frequency normal modes to enforce collective movements in refining macromolecular structural models. *Proc. Natl. Acad. Sci. USA* **2004**, *101*, 6957–6962. [CrossRef] [PubMed]

94. Lu, M.; Ma, J. The role of shape in determining molecular motions. *Biophys. J.* **2005**, *89*, 2395–2401. [CrossRef]

95. Doruker, P.; Jernigan, R.L.; Bahar, I. Dynamics of large proteins through hierarchical levels of coarse-grained structures. *J. Comput. Chem.* **2002**, *23*, 119–127. [CrossRef]

96. Doruker, P.; Jernigan, R.L. Functional motions can be extracted from on-lattice construction of protein structures. *Proteins* **2003**, *53*, 174–181. [CrossRef]

97. Kurkcuoglu, O.; Jernigan, R.L.; Doruker, P. Mixed levels of coarse-graining of large proteins using elastic network model succeeds in extracting the slowest motions. *Polymer* **2004**, *45*, 649–657. [CrossRef]

98. Zheng, W.; Brooks, B.R.; Thirumalai, D. Low-frequency normal modes that describe allosteric transitions in biological nanomachines are robust to sequence variations. *Proc. Natl. Acad. Sci. USA* **2006**, *103*, 7664–7669. [CrossRef] [PubMed]

99. Poma, A.B.; Li, M.S.; Theodorakis, P.E. Generalization of the elastic network model for the study of large conformational changes in biomolecules. *Phys. Chem. Chem. Phys.* **2018**, *20*, 17020–17028. [CrossRef] [PubMed]

100. Higo, J.; Umeyama, H. Protein dynamics determined by backbone conformation and atom packing. *Protein Eng.* **1997**, *10*, 373–380. [CrossRef]

101. Chng, C.-P.; Yang, L.-W. Coarse-grained models reveal functional dynamics—II. Molecular dynamics simulation at the coarse-grained level—Theories and biological applications. *Bioinform. Biol. Insights* **2008**, *2*, 171–185. [CrossRef] [PubMed]

102. Gur, M.; Madura, J.D.; Bahar, I. Global transitions of proteins explored by a multiscale hybrid methodology: Application to adenylate kinase. *Biophys. J.* **2013**, *105*, 1643–1652. [CrossRef] [PubMed]

103. Cressman, A.; Togashi, Y.; Mikhailov, A.S.; Kapral, R. Mesoscale modeling of molecular machines: Cyclic dynamics and hydrodynamical fluctuations. *Phys. Rev. E* **2008**, *77*, 050901. [CrossRef] [PubMed]

104. Echeverria, C.; Togashi, Y.; Mikhailov, A.S.; Kapral, R. A mesoscopic model for protein enzymatic dynamics in solution. *Phys. Chem. Chem. Phys.* **2011**, *13*, 10527–10537. [CrossRef] [PubMed]

105. Echeverria, C.; Kapral, R. Molecular crowding and protein enzymatic dynamics. *Phys. Chem. Chem. Phys.* **2012**, *14*, 6755–6763. [CrossRef] [PubMed]

106. Schofield, J.; Inder, P.; Kapral, R. Modeling of solvent flow effects in enzyme catalysis under physiological conditions. *J. Chem. Phys.* **2012**, *136*, 205101. [CrossRef]

107. Echeverria, C.; Kapral, R. Diffusional correlations among multiple active sites in a single enzyme. *Phys. Chem. Chem. Phys.* **2014**, *16*, 6211–6216. [CrossRef]

108. Takano, M.; Terada, T.P.; Sasai, M. Unidirectional Brownian motion observed in an in silico single molecule experiment of an actomyosin motor. *Proc. Natl. Acad. Sci. USA* **2010**, *107*, 7769–7774. [CrossRef]

109. Avetisov, V.A.; Ivanov, V.A.; Meshkov, D.A.; Nechaev, S.K. Fractal globules: A new approach to artificial molecular machines. *Biophys. J.* **2014**, *107*, 2361–2368. [CrossRef] [PubMed]

110. Fernández, J.D.; Vico, F.J. Automating the search of molecular motor templates by evolutionary methods. *BioSystems* **2011**, *106*, 82–93. [CrossRef]

111. Sarkar, A.; Flechsig, H.; Mikhailov, A.S. Towards synthetic molecular motors: A model elastic-network study. *New J. Phys.* **2016**, *18*, 043006. [CrossRef]

112. Flechsig, H. Design of elastic networks with evolutionary optimised long-range communication as mechanical models of allosteric proteins. *Biophys. J.* **2017**, *113*, 558–571. [CrossRef] [PubMed]

113. Flechsig, H.; Togashi, Y. Designed elastic networks: Models of complex protein machinery. *Int. J. Mol. Sci.* **2018**, *19*, 3152. [CrossRef] [PubMed]

114. Wang, Y.; Rader, A.J.; Bahar, I.; Jernigan, R.L. Global ribosome motions revealed with elastic network model. *J. Struct. Biol.* **2004**, *147*, 302–314. [CrossRef] [PubMed]

115. Ramaswamy, A.; Bahar, I.; Ioshikhes, I. Structural dynamics of nucleosome core particle: Comparison with nucleosomes containing histone variants. *Proteins* **2005**, *58*, 683–696. [CrossRef] [PubMed]

116. Isami, S.; Sakamoto, N.; Nishimori, H.; Awazu, A. Simple elastic network models for exhaustive analysis of long double-stranded DNA dynamics with sequence geometry dependence. *PLoS ONE* **2015**, *10*, e0143760. [CrossRef] [PubMed]

117. Kameda, T.; Isami, S.; Togashi, Y.; Nishimori, H.; Sakamoto, N.; Awazu, A. The 1-particle-per-k-nucleotides (1PkN) elastic network model of DNA dynamics with sequence-dependent geometry. *Front. Physiol.* **2017**, *8*, 103. [CrossRef]

118. Sauerwald, N.; Zhang, S.; Kingsford, C.; Bahar, I. Chromosomal dynamics predicted by an elastic network model explains genome-wide accessibility and long-range couplings. *Nucleic Acids Res.* **2017**, *45*, 3663–3673. [CrossRef] [PubMed]

119. Ohmura, I.; Morimoto, G.; Ohno, Y.; Hasegawa, A.; Taiji, M. MDGRAPE-4: A special-purpose computer system for molecular dynamics simulations. *Phil. Trans. R. Soc. A* **2014**, *372*, 20130387. [CrossRef] [PubMed]

120. Kamiya, K.; Sugawara, Y.; Umeyama, H. Algorithm for normal mode analysis with general internal coordinates. *J. Comput. Chem.* **2003**, *24*, 826–841. [CrossRef] [PubMed]

121. Lopéz-Blanco, J.R.; Garzón, J.I.; Chacón, P. iMod: Multipurpose normal mode analysis in internal coordinates. *Bioinformatics* **2011**, *27*, 2843–2850. [CrossRef]